

**Nonlinear parametric oscillator: A tool for probing quantum fluctuations**

Prasun Sarkar\* and Jayanta K. Bhattacharjee

*Indian Association for the Cultivation of Science, Jadavpur, Kolkata-700 032, India*

(Received 16 June 2020; accepted 15 October 2020; published 4 November 2020)

Nanomechanical oscillators have, over the last few years, started probing regimes where quantum fluctuations are important. Here we consider a nonlinear parametric oscillator in the quantum domain. We show that in the classical subharmonic resonance zone, the quantum fluctuations are finite but greatly magnified depending on the strength of the nonlinear coupling. This should make such oscillators useful in probing quantum fluctuations.

DOI: [10.1103/PhysRevE.102.052204](https://doi.org/10.1103/PhysRevE.102.052204)**I. INTRODUCTION**

The emergence of nanoscale devices [1–6] which feature various kinds of nonlinear mechanical oscillators has made it worthwhile to study the quantum dynamics of such systems. Since these devices as yet are on the verge of onset of quantum effects [7–12], it makes sense to explore the first effect of quantum fluctuations on such systems. Parametrically driven simple harmonic oscillators, governed by the Hamiltonian  $H = \frac{p^2}{2m} + \frac{1}{2}m\omega^2x^2(1 + \epsilon \cos \Omega t)$ , have long been essential in the field of ion trapping [13] and have been extensively studied [14–17]. The classical dynamics governed by this Hamiltonian is described by the Mathieu equation and has striking properties. The equation shows divergent subharmonic response [18] in a narrow zone around  $\omega = \Omega/2$  (primary response) in the  $\epsilon$  versus  $\omega$  plane with secondary strong responses in narrower zones around  $\omega = n\Omega/2$ , where  $n = 2, 3, 4, \dots$ . The particle concerned is supposed to wander off to infinity in these resonance zones. While the existence of the primary resonance was well known (the technique of increasing the amplitude of oscillations of the playground swing [19]), the first clear evidence of existence of the higher resonances was provided by Turner *et al.* [20]. Subsequently, the nonlinear dynamics of microelectronic and nanoelectronic mechanical oscillators (MEMS and NEMS) have been extensively investigated to probe the curious behavior of parametrically and directly driven nonlinear systems [21–26]. A particularly intriguing application is to the study of the Casimir effect [27]. A detailed review of these theoretical and experimental contributions can be found in Refs. [28,29].

Investigation of the quantum parametric oscillator also has a long history. The Floquet functions and the Floquet energies were calculated by Perelomov and Pelov [30] showing a discrete spectrum in the classical stable zone and a continuous one in the unstable region. The propagator for the system (for an initial Gaussian wave packet) was obtained subsequently by various authors [31–33]. The primary use of the nonlinear quantum parametric oscillator at the early phase was in the

study of quantum optics. One of the earliest studies was by Graham and Haken [34]. The issue of quantum noise in these systems was addressed by Carmichael and Wolinsky [35]. Dynamical calculations for the quantum parametric oscillator using a coherent state basis was carried out by Kinsler and Drumond [36]. More recently, a nonlinear parametric oscillator was studied by Ding *et al.* [37] who considered two similar ions in a linear Paul trap with the nonlinearity provided by the Coulomb interaction among the ions. Of particular importance in our context is the work of Dykman *et al.* [38] and Peano and Dykman [39], where a rotating wave transformation is used to generate a new Hamiltonian whose quasi-energies can be studied.

In the early studies of quantum dynamics associated with the above Hamiltonian, however, the focus has usually not been on the instability zone. As stated clearly in the path integral treatment [16], the focus is on reducing the problem to an effective simple harmonic oscillator modeled by a static Hamiltonian. Our aim in this work is to use the dynamics of quantum averages to understand the evolution of the average values of relevant dynamical variables. In the quantum oscillator it is not sufficient to study the dynamics of the mean position but also the higher moments which are the essential features of a quantum system. The second moment which is the variance  $V = \langle x^2 \rangle - \langle x \rangle^2 = \langle (x - \langle x \rangle)^2 \rangle$  is the absolutely nonignorable part of the quantum dynamics and is directly related to the energy of the quadratic Hamiltonian considered above. The mean position  $\langle x \rangle$  follows exactly the Mathieu equation written above and shows the same instability zones as in the case of the classical problem. The immediate question is whether the variance has divergence zones as well. Recent publications [40–42] have revealed two interesting facts about this system:

(1) The instability zones of both  $\langle x \rangle$  and  $V$  originate from the same points on the frequency axis in the  $\omega$ - $\epsilon$  plane, i.e.,  $\omega = n\frac{\Omega}{2}$  ( $n = 1, 2, 3, \dots$ ).

(2) The instability zones are completely identical. In Refs. [40] and [42] the *skewness* and *kurtosis* have been studied as well.

In real systems, particles never wander off to infinity. If they stray too far from the center then the nonlinear terms in the Hamiltonian become important and a small amount

\*Corresponding author: [pcps@iacs.res.in](mailto:pcps@iacs.res.in)

of nonlinearity restricts the final amplitude to a large but finite value. This is a natural phenomenon in molecular binding where the effective potential binding the atoms is of a Lennard-Jones  $V(x) = V_0[(\frac{a}{x})^{12} - (\frac{a}{x})^6]$  or Morse  $V(x) = V_0[-1 + (1 - e^{-ax})^2]$  variety, and these have a minima at some value  $x = x_0$ . Expansion around  $x = x_0$  gives quadratic and higher order terms. An additional restoring term in the Hamiltonian that has led to the largest amount of investigation corresponds to a cubic restoring force. The Hamiltonian is now

$$H = \frac{p^2}{2m} + \frac{1}{2}m\omega^2x^2(1 + \epsilon \cos \Omega t) + \frac{m\lambda}{4}x^4. \quad (1)$$

The quartic term is small for displacements of the order of angstroms. In an oxygen molecule, its contribution to the vibrational ground state energy is less than 0.1% of the quadratic term. It increases with the quantum number  $n$  and for  $n \simeq 100$  (semiclassical) can be a significant effect [43]. The corresponding classical dynamics as given by  $\ddot{x} = -\omega^2(1 + \epsilon \cos \Omega t)x - \lambda x^3$  has been well studied [25,44]. The primary resonance zone (here the response is subharmonic and of finite but large amplitude proportional to  $\lambda^{-1/2}$ ) is around  $\omega = \Omega/2$  and the zone is  $(\epsilon \ll 1) - \epsilon\Omega/8 < \delta < \epsilon\Omega/8$ , where  $\omega = \frac{\Omega}{2} + \delta$ . These results can be obtained analytically from the fixed points of the Krylov-Bogoliubov flow equations. We use the Krylov-Bogoliubov scheme here because it gives a direct route to the slow flow dynamics. Identical results could have been obtained by using the two timescales method or even a judicious combination of harmonic balance and the Linstedt-Poincaré technique [45–47].

In this work we focus on the quantum dynamics ensuing from the Hamiltonian of Eq. (1) in the weak quantum limit [48–54] where the variance is small and the kurtosis and higher moments are treated in a Gaussian approximation. Our principal findings are the following:

(1) The trivial fixed point of the Krylov-Bogoliubov flow equations are stable for  $\delta > \Omega/8$ , and the dynamics is a low-amplitude oscillation about the trivial fixed point.

(2) The nontrivial fixed points of the Krylov-Bogoliubov flow are completely wiped out by quantum fluctuations.

(3) Nevertheless, there is a finite but large-amplitude quasiperiodic dynamics of both the mean position and the variance in the classical instability zone.

We organize the present paper as follows: In Sec. II we present a derivation of the quantum dynamics in the weak quantum limit. In Sec. III we discuss how the model can be treated in a standard nonlinear dynamics framework with the help of Krylov-Bogoliubov method. In Sec. IV we solve the model numerically and conclude the present work with a short summary in Sec. V.

## II. THE QUANTUM MODEL

We begin with a derivation of our dynamical system, using the Heisenberg equation of motion for the expectation value of an operator (Ehrenfest's theorem),

$$\frac{d}{dt}\langle O \rangle = \frac{\partial}{\partial t}\langle O \rangle + \frac{1}{i\hbar}\langle [O, H] \rangle, \quad (2)$$

where  $H$  is the Hamiltonian given in Eq. (1).

Two derivatives for the position operator lead to

$$\frac{d^2}{dt^2}\langle x \rangle = -\omega^2 f(t)\langle x \rangle - \lambda\langle x^3 \rangle, \quad (3)$$

where  $f(t) = 1 + \epsilon \cos \Omega t$ . We note that  $\langle x^3 \rangle = \langle x \rangle^3 + 3V\langle x \rangle + S$  where  $S = \langle (x - \langle x \rangle)^3 \rangle$  is the *skewness*. We simplify the calculations by working with initial wave packets which have  $S = 0$  and by assuming that under the symmetric Hamiltonian, the  $S = 0$  situation will be maintained. Thus, the dynamics of the mean position is

$$\frac{d^2}{dt^2}\langle x \rangle = -\omega^2 f(t)\langle x \rangle - \lambda\langle x \rangle^3 - 3\lambda V\langle x \rangle. \quad (4)$$

To find the dynamics of the variance, we write

$$\begin{aligned} \frac{d^2}{dt^2}\langle x^2 \rangle &= \frac{1}{m} \frac{d}{dt}\langle xp + px \rangle = \frac{1}{m} \left\langle \left[ \frac{(xp + px)}{i\hbar}, H \right] \right\rangle \\ &= \frac{2}{m^2}\langle p^2 \rangle - 2\omega^2 f(t)\langle x^2 \rangle - 2\lambda\langle x^4 \rangle. \end{aligned} \quad (5)$$

Similarly,

$$\frac{d^2}{dt^2}\langle x^2 \rangle = \frac{2}{m^2}\langle p \rangle^2 - 2\omega^2 f(t)\langle x \rangle^2 - 2\lambda\langle x^3 \rangle\langle x \rangle. \quad (6)$$

We thus obtain

$$\begin{aligned} \frac{d^2V}{dt^2} &= \frac{d^2}{dt^2}(\langle x^2 \rangle - \langle x \rangle^2) \\ &= \frac{2}{m^2}\langle (\Delta p)^2 \rangle - 2\omega^2 f(t)V - 2\lambda[\langle x^4 \rangle - \langle x^3 \rangle\langle x \rangle] \\ &= \frac{2}{m^2}\langle (\Delta p)^2 \rangle - 2\omega^2 f(t)V - 2\lambda[K + 3V\langle x \rangle^2]. \end{aligned} \quad (7)$$

In the last line, we have assumed  $S = 0$  and  $K$  stands for the kurtosis  $\langle (x - \langle x \rangle)^4 \rangle$ . Long but straightforward algebra gives

$$\frac{d}{dt}\langle (\Delta p)^2 \rangle = -m^2\omega^2 f(t)\frac{dV}{dt} - \frac{m^2\lambda}{2}\left[\frac{d}{dt}\langle x^4 \rangle - 4\langle x^3 \rangle\frac{d\langle x \rangle}{dt}\right]. \quad (8)$$

Using the assumption  $S = 0$  and noting that  $\langle x^4 \rangle = K + 6V\langle x \rangle^2 + \langle x \rangle^4$ , where  $K$  is the *kurtosis*, we finally arrive at the dynamics

$$\begin{aligned} \frac{d^3V}{dt^3} + 4\omega^2 f(t)\frac{dV}{dt} &= -2\omega^2 \frac{df}{dt}V - 12\lambda\langle x \rangle^2 \frac{dV}{dt} \\ &\quad - 6\lambda V \frac{d}{dt}\langle x \rangle^2 - 3\lambda \frac{dK}{dt}. \end{aligned} \quad (9)$$

Our closed-form expression of the dynamical system is obtained if we use a Gaussian closure to write  $K = 3V^2$  and obtain from Eq. (9)

$$\begin{aligned} \frac{d^3V}{dt^3} + 4\omega^2 f(t)\frac{dV}{dt} &= -2\omega^2 \frac{df}{dt}V - 12\lambda\langle x \rangle^2 \frac{dV}{dt} \\ &\quad - 6\lambda V \frac{d}{dt}\langle x \rangle^2 - 9\lambda \frac{dV^2}{dt}. \end{aligned} \quad (10)$$

The two nonlinear coupled differential equations for  $\langle x \rangle$  and  $V$  [Eq. (4) and Eq. (10)] constitute our dynamical system. At this juncture, it is convenient to imagine all frequencies

to have been scaled by the characteristic frequency  $\omega_0$  of the system and all lengths to have been scaled by the characteristic length  $l_0$  of the system. The nonlinearity parameter then becomes the dimensionless variable  $\bar{\lambda} = \lambda l_0^2 / \omega_0^2$ . The fact that we have made Eqs. (4) and (10) constitute a closed dynamical system essentially means that terms containing  $\hbar$  explicitly have been dropped, and the variance  $V$  and  $\langle x \rangle^2$  are small in the sense that  $\lambda V / \omega^2$  and  $\lambda \langle x \rangle^2 / \omega^2$  are small and the higher moments are all obtained from  $\langle x \rangle$  and  $V$  by the Gaussian distribution constraint. This essentially defines the weak quantum limit.

At this point, it is important to explain how our procedure differs from the conventional semiclassical approach taken in Refs. [48–53]. In these contributions, the point of view is to look at classical dynamics from the Liouville approach of starting with multiple initial conditions in phase space and then letting the time evolution lead to spreading out of trajectories which allows for the calculation of average values and deviations therefrom. These averages are compared with the naturally occurring quantum averages and fluctuations. The correspondence exists for a short time interval and is supposed to break down beyond a characteristic time. A very detailed investigation of this has been carried out in Katz *et al.* [55] for the driven Duffing oscillator. These authors find that in the early stages of evolution, the quantum Wigner function and the classical phase-space distributions agree well with each other. An agreement between quantum observables and classical averages was also observed, but no particular timescale for the agreement was seen. Our point of view is to look for quantum averages only, which for linear systems is absolutely straightforward (for all moments) but for nonlinear systems gives rise to a hierarchy. The dynamics of the expectation values  $\langle x \rangle$  (position) and  $\langle p \rangle$  (momentum) couple at least to the variance  $V$  and as shown in our case to  $V$  and  $S$  (depending on the nonlinearity, even higher orders may be involved). The dynamics of  $V$  in turn couples to higher moments like kurtosis ( $K$ ), and one has an infinite order system. This happens in all cases of Galerkin truncation of a nonlinear partial differential equation. To deal with such situations, closure schemes were developed [32,33] where higher order moments were expressed in terms of lower order moments and the approximation that we have used here is the most frequently used one in that context. In this approach, attention is focused on long-time solutions—the usual goal in a dynamical system—and hence what we will be looking at is long-time behavior of the dynamical variables.

A very important quantity that we have not discussed so far is the average energy. In general, for an autonomous system, the average energy (expectation value of the Hamiltonian) is a constant of motion and thus helps in keeping track of the dynamics, described above. However, for the time-dependent Hamiltonian that we are discussing here [Eq. (1), the energy is not a constant of motion. In fact, using Eq. (2), its rate of change is governed by

$$\begin{aligned} \frac{dE}{dt} &= \frac{d}{dt} \langle H \rangle = -\epsilon m \omega^3 \langle x^2 \rangle \sin \omega t \\ &= -\epsilon m \omega^3 [V + \langle x \rangle^2] \sin \omega t. \end{aligned}$$

The right-hand side would average out to zero, over a period  $2\pi/\omega$  if  $\langle x^2 \rangle$  happens to be a constant. If  $\langle x^2 \rangle$  (in reality the  $V$  part of it) is periodic, with a period different from  $2\pi/\omega$ , then it could be nonzero and significant. What we will find in the next section is that it has a complicated time dependence which can provide a small contribution to the average growth rate of the energy, if averaged over  $2\pi/\omega$ . This could be the signature of the quantum heating found by Dykman *et al.* [38] in the parametrically modulated oscillator and later in the driven Duffing oscillator [39]. It should be noted that comparison with Dykman *et al.* [38,39] is valid only in the limit of the bath temperature  $T$  tending to zero.

Our coupled dynamical system of Eqs. (4) and (10) do not reveal very much—in particular, because they form a nonautonomous system. We will need to solve the system numerically to arrive at the true picture. This will be done in Sec. IV. To get some insight, however, we will carry out the standard simplifying technique of working with systems as represented by Eqs. (4) and (10). The linearized system in both cases is a Mathieu oscillator with a very strong response when  $\omega$  is close to  $\Omega/2$  (primary resonance). Accordingly, we will carry out this simplification in Sec. III and see what insight we can gather from this process.

### III. A KRYLOV-BOGOLIUBOV TREATMENT

Since the subharmonic response of  $\langle x \rangle$  at  $\omega = \Omega/2$  is the most spectacular classical limit associated with Eqs. (4) and (10), we focus on this in the quantum case and add the concomitant variance dynamics which has to feature a periodic response of frequency  $\Omega$  as is obvious from the nonlinear terms and is also known from the study of the quantum Mathieu equation [40]. Accordingly we embark on a Krylov-Bogoliubov procedure with the choice

$$\langle x \rangle = A \cos \frac{\Omega t}{2} + B \sin \frac{\Omega t}{2}$$

$$\text{and } V(t) = V_0(t) + V_1(t) \cos \Omega t + V_2(t) \sin \Omega t. \quad (11)$$

Interestingly, this procedure for the dynamical system is analogous to the rotating wave approximation [canonical transformation by  $u_1 = \exp(-ia^\dagger a \omega t/2)$  where  $a^\dagger$  and  $a$  are the creation and annihilation operators] carried out by Dykman *et al.* [38] on the Hamiltonian itself. It should be noted that the new Hamiltonian in Ref. [38] did not have the form of a sum of kinetic and potential energies, and we will see the counterpart of that in our case.

For  $\epsilon = 0$ ,  $V_0, V_1, V_2$  are constants, and hence we assume for  $\epsilon \neq 0$ , all of them  $A, B, V_0, V_1, V_2$  are slowly varying functions of time and only the first derivatives [of the order of  $\epsilon$  i.e.,  $O(\epsilon)$ ] appear in the flow. We work near  $\omega = \frac{\Omega}{2}$  and consider frequencies  $\omega = \frac{\Omega}{2} + \epsilon\delta$ . The flow equations are

$$\begin{aligned} \dot{A} &= \epsilon \left( \delta - \frac{\Omega}{8} \right) B + \frac{3\lambda}{4\Omega} B(A^2 + B^2) \\ &\quad + \frac{3\lambda}{\Omega} B V_0 + \frac{3\lambda}{2\Omega} (A V_2 - B V_1), \end{aligned} \quad (12a)$$

$$\begin{aligned} \dot{B} &= -\epsilon \left( \delta + \frac{\Omega}{8} \right) A - \frac{3\lambda}{4\Omega} A(A^2 + B^2) \\ &\quad - \frac{3\lambda}{\Omega} A V_0 - \frac{3\lambda}{2\Omega} (A V_1 + B V_2), \end{aligned} \quad (12b)$$

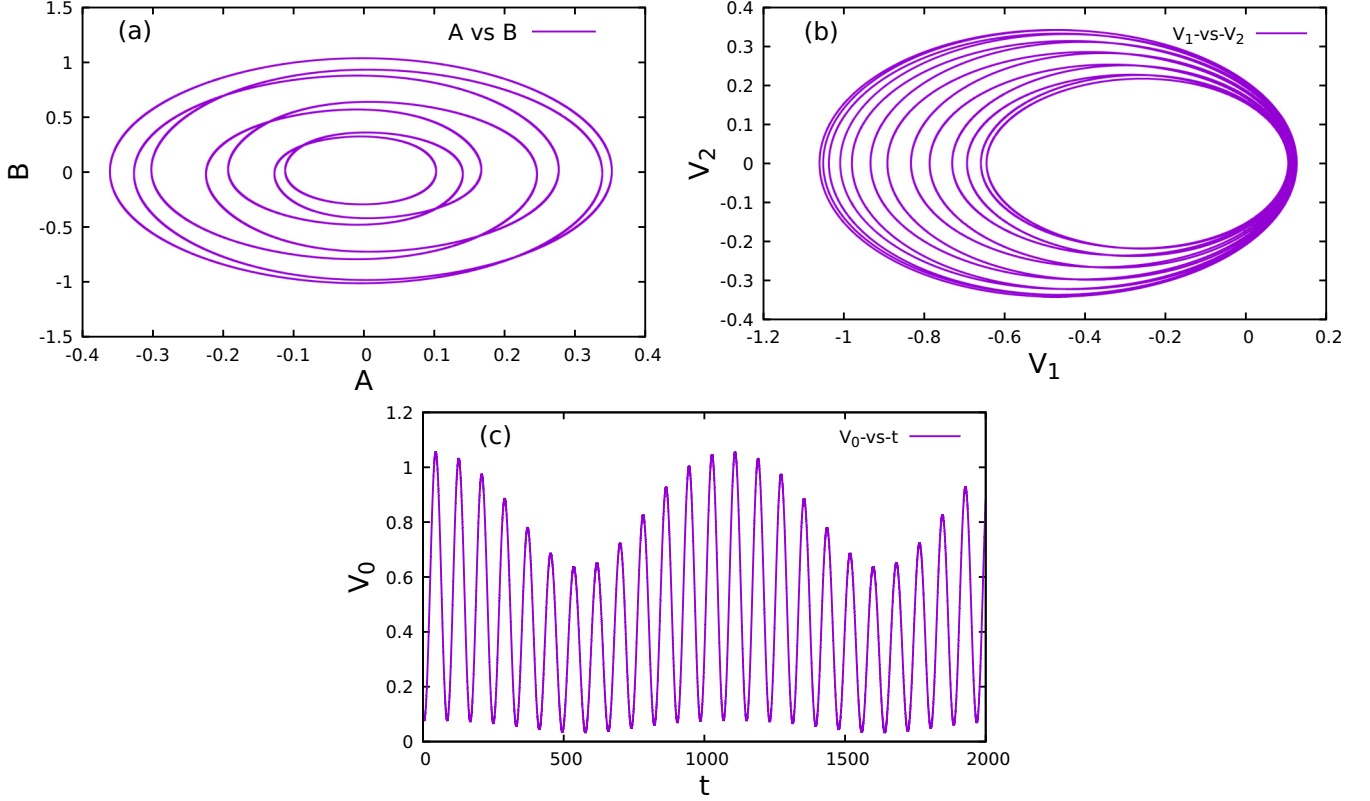


FIG. 1. Phase portraits and time series plots obtained from the Krylov-Bogoliubov flow in Region III (stable zone). For instance  $A$  vs  $B$  is shown in panel (a) and corresponds to a bounded but aperiodic orbit. In panel (b)  $V_1$  vs  $V_2$  has been drawn, which is similar to the  $A$  vs  $B$  plot. The time series for  $V_0$  is shown in panel (c) and shows bounded oscillations which are not periodic. In all cases, the amplitudes are  $O(1)$ . The parameters used are  $\Omega = 4.0$ ,  $\delta = 0.60$ ,  $\epsilon = 0.11$ ,  $\bar{\lambda} = 0.001$  ( $A, B$  are in units of  $l_0$ ,  $V_0, V_1$  and  $V_2$  are in units of  $l_0^2$ , and  $\Omega$  and  $\delta$  are in units of  $\omega_0$  and  $\bar{\lambda} = \lambda l_0^2 / \omega_0^2$ ).

$$\dot{V}_0 = -\frac{\epsilon\Omega}{4}V_2 - \frac{3\lambda}{2\Omega}(A^2 - B^2)V_2 + \frac{3\lambda}{\Omega}ABV_1, \quad (12c)$$

$$\dot{V}_1 = \left[2\epsilon\delta + \frac{3\lambda}{\Omega}(A^2 + B^2)\right]V_2 + \frac{3\lambda}{\Omega}ABV_0 + \frac{9\lambda}{\Omega}V_0V_2, \quad (12d)$$

$$\begin{aligned} \dot{V}_2 = & -\left[2\epsilon\delta + \frac{3\lambda}{\Omega}(A^2 + B^2)\right]V_1 \\ & - \left[\frac{\epsilon\Omega}{4} + \frac{3\lambda}{2\Omega}(A^2 - B^2)\right]V_0 - \frac{9\lambda}{\Omega}V_0V_1. \end{aligned} \quad (12e)$$

In the classical limit, the  $V$ 's are absent, and we have the dynamics given by Eq. (12a) and Eq. (12b) with  $A$  and  $B$  only. The trivial fixed point is  $(0, 0)$ . It is a center for  $\delta > \Omega/8$  (henceforth we will call this parameter range “Region III”) and unstable for  $\delta < \Omega/8$ . The domain  $\frac{\Omega}{8} > \delta > -\frac{\Omega}{8}$  will be called “Region II.” In Region III, one sees low-amplitude (determined by initial conditions) slow oscillations in  $A$  and  $B$ . For  $\delta < \Omega/8$ , in Region II, the stable solution is  $A = 0$  and  $B^2 = \frac{4\Omega}{3\lambda}(\frac{\Omega}{8} - \delta)$ , which corresponds to a large-amplitude oscillation for  $\bar{\lambda} \ll 1$ . The nature of the solution changes completely for  $\delta < -\Omega/8$  (Region I). These are the well-known solutions for the classical situation [44].

At this point, it is very important to compare our results with that of Dykman *et al.* [38] and the earlier work of Dykman and Smelyanskiy [56], Dykman [57], and, in particular, Marthaler and Dykman [58]. In Ref. [58], it has been shown that the rotating wave approximation takes the original coordinates, the  $x$  and  $p$  of the Hamiltonian, in Eq. (1) to the mixed variables  $Q$  and  $P$  in terms of which the equations of motion read  $\dot{Q} = (1 - \mu)P + P(P^2 + Q^2)$  and  $\dot{P} = (1 + \mu)Q - Q(P^2 + Q^2)$ . This is precisely our Eqs. (12a) and (12b) with  $V_0 = V_1 = V_2 = 0$ , i.e., neglecting the effect of quantum variance. The dynamics is almost like that in a double-well potential centered at  $B = \pm\sqrt{\frac{4\Omega\epsilon}{3\lambda}(\frac{\Omega}{8} - \delta)}$ . In Ref. [38] the authors subsequently consider the addition of an external noise and write a Markovian dynamics in their Eq. (5). However, in Sec. III of the paper, they consider the very small damping (external noise) limit and still find a “noise” which is characterized by what is termed as quantum temperature. In our case, the role of the quantum temperature is triggered by the quantum variance, which effectively generates “noise” in the system.

We now include the quantum fluctuations characterized by the variance and ask for the new trivial fixed point. This gives a line of fixed points  $A = 0$ ,  $B = 0$ ,  $V_2 = 0$ , and  $V_1 + \frac{\Omega}{8\delta}V_0 + \frac{9\lambda}{2\epsilon\delta\Omega}V_0V_1 = 0$ . Since the variance  $V$  has to be greater than zero at any instant of time we must have  $\delta > \Omega/8$ , and

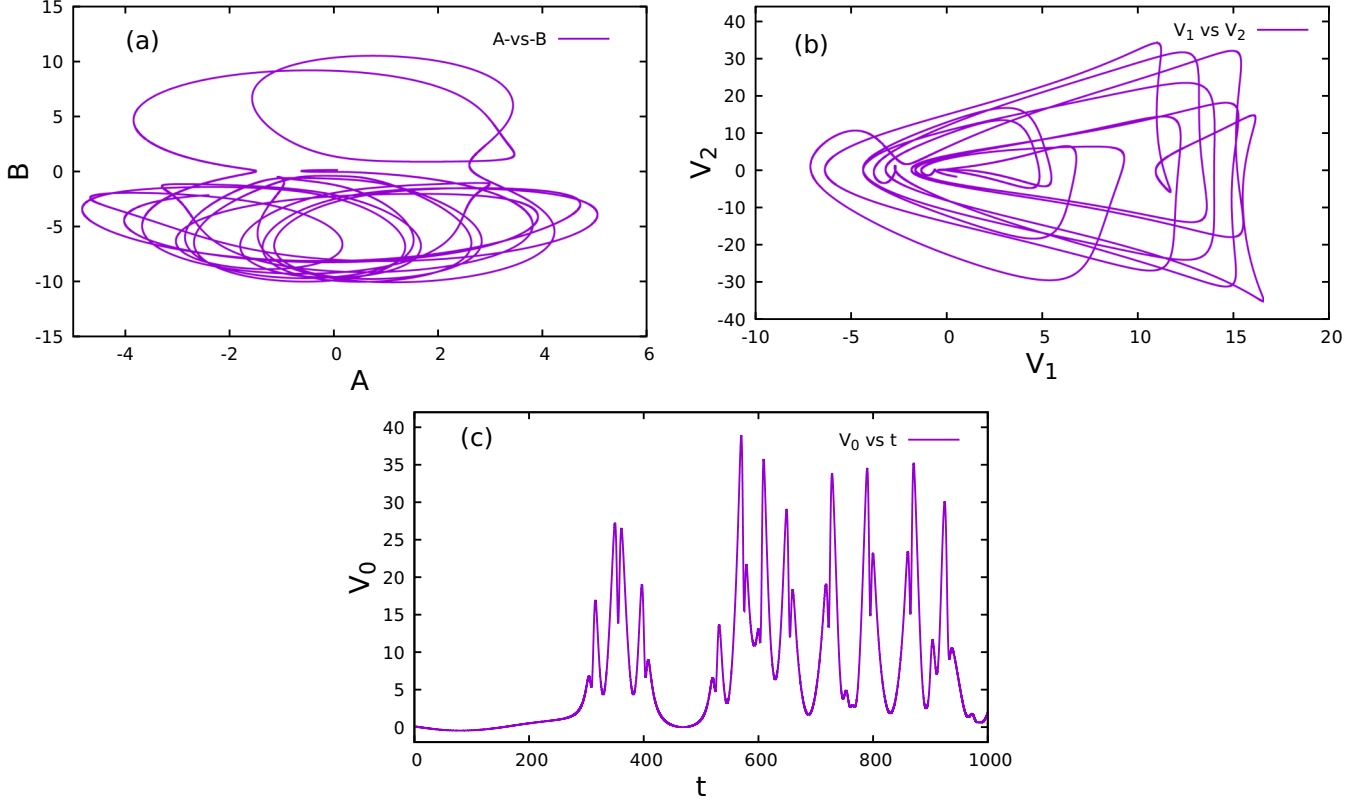


FIG. 2. Phase portraits and time series plots for the Krylov–Bogoliubov flow in Region II (resonance zone) showing a complete absence of periodic or quasiperiodic behavior. For instance,  $A$  vs  $B$  is shown in panel (a). In panel (b),  $V_1$  vs  $V_2$  is drawn, while the time series for  $V_0$  is shown in panel (c). The parameters used in solving the flow equations are:  $\Omega = 4.0$ ,  $\delta = -0.10$ ,  $\epsilon = 0.11$ ,  $\lambda = 0.001$  (units as in Fig. 1). In comparison with Fig. 1, two things need to be noted: the large amplitudes of the dynamics and the absence of regularity.

that is the region (Region III) where this fixed point exists. Hence the trivial quantum “fixed point” is actually a fixed line. The fluctuations smear the point into a line. It is stable, which can be easily ascertained from a linearization of Eq. (12a) to Eq. (12e) around this condition. These statements are corroborated by a numerical simulation of Eqs. (12) as shown in Fig. 1. In Fig. 1 we are at  $\delta = 0.60$ , which is greater than  $\Omega/8$ . Figure 1(a) shows that the trajectory winds round in the  $A$ - $B$  plane about the fixed point  $A = B = 0$ , which is a center. In Fig. 1(b) we show the time development in the  $V_1$ - $V_2$  plane. The winding occurs around  $V_2 = 0$  and a nonzero negative value of  $V_1$ . The time series  $V_0(t)$  is displayed in Fig. 1(c).

We have just seen that the quantum fluctuations smear out the stable fixed point  $A = B = 0$  in Region III (i.e.,  $\delta > \Omega/8$ ) and give rise to a fixed line. The dynamics, however, remains almost periodic and low amplitude and is not of particular interest. It is in Region II ( $-\Omega/8 < \delta < \Omega/8$ ) that the parametric oscillation effects are very strong, and to get the first effect of the fluctuations (the variance  $V$ ), we simply consider  $V$  as a parameter, represented by  $V_0$ , with

$V_1 = V_2 = 0$ . The effect of the variance is to change Eqs. (12a) and (12b) to

$$\dot{A} = \left[ \epsilon \left( \delta - \frac{\Omega}{8} \right) + \frac{3\lambda}{\Omega} V_0 \right] B + \frac{3\lambda}{4\Omega} B(A^2 + B^2), \quad (13a)$$

$$\dot{B} = - \left[ \epsilon \left( \delta + \frac{\Omega}{8} \right) + \frac{3\lambda}{\Omega} V_0 \right] A - \frac{3\lambda}{4\Omega} A(A^2 + B^2). \quad (13b)$$

The nontrivial fixed point  $A = 0$ ,  $B^2 = \frac{4\Omega}{3\lambda} \left[ \epsilon \left( \frac{\Omega}{8} - \delta \right) - \frac{3\lambda V_0}{\Omega} \right]$  exists only if  $\epsilon \left( \frac{\Omega}{8} - \delta \right) > \frac{3\lambda V_0}{\Omega}$ , and we see the quantum fluctuations trying to “erase” the fixed points which gave the effect of a double-well potential. This is a milder version of the result in Ref. [38], where the effect of the fluctuations is to make the equispaced energy levels unequally spaced. Here, if  $V_0$  is smaller than a critical value  $V_{0c} = \frac{\Omega \epsilon}{3\lambda} \left( \frac{\Omega}{8} - \delta \right)$ , the levels are still equispaced with a smaller spacing but then for  $V_0 > V_{0c}$ , the harmonic well is no longer there.

For  $\delta < \Omega/8$  in Region II, we now show that the quantum fluctuations prevent the existence of any fixed point. We use  $A = R \sin \theta$  and  $B = R \cos \theta$  to write the fixed point conditions coming from Eq. (12a) to Eq. (12e) as

$$\left[ \epsilon \Omega \left( \delta - \frac{\Omega}{8} \right) + 3\lambda \left( V_0 - \frac{1}{2} V_1 \right) + \frac{3\lambda}{4} R^2 \right] \cos \theta + \frac{3\lambda}{2} V_2 \sin \theta = 0, \quad (14a)$$

$$\left[ \epsilon \Omega \left( \delta + \frac{\Omega}{8} \right) + 3\lambda \left( V_0 + \frac{1}{2} V_1 \right) + \frac{3\lambda}{4} R^2 \right] \sin \theta + \frac{3\lambda}{2} V_2 \cos \theta = 0, \quad (14b)$$

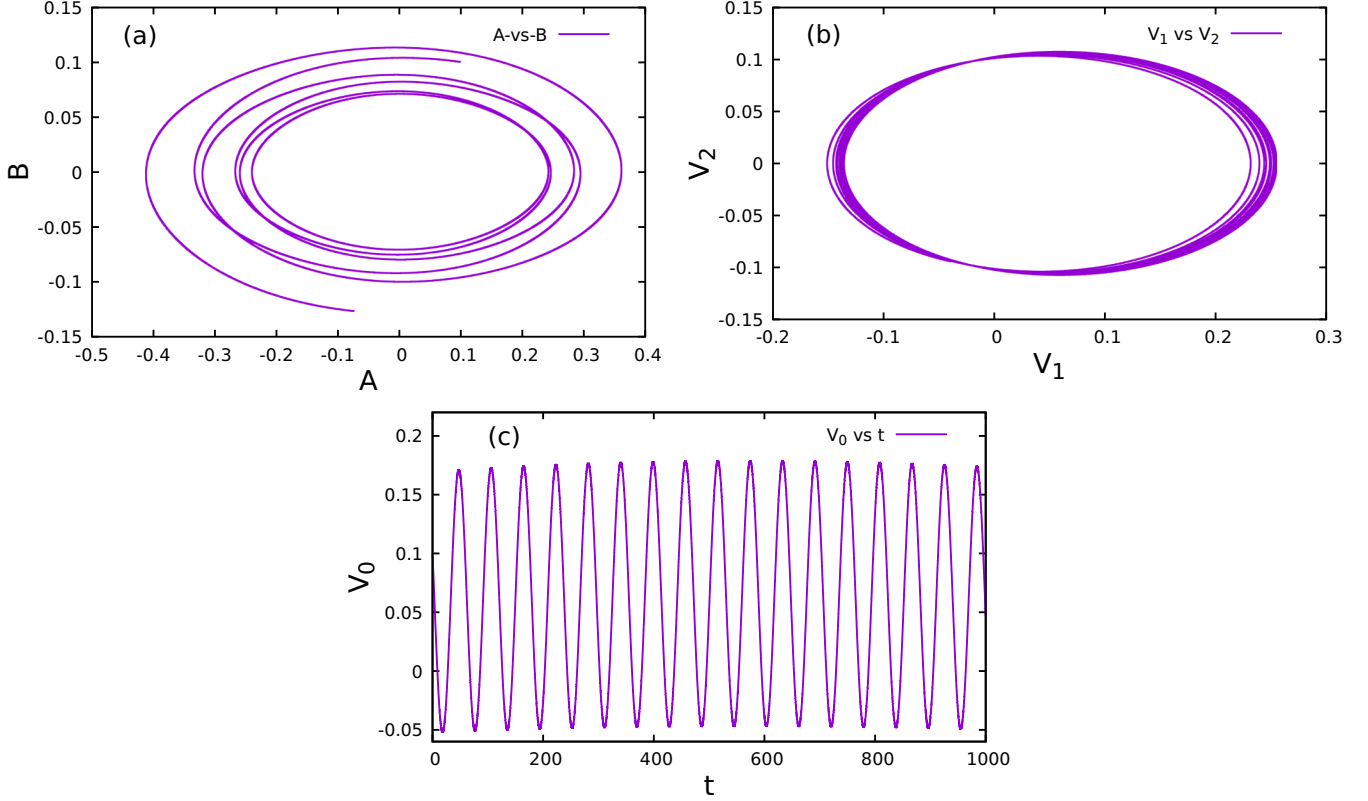


FIG. 3. Phase portraits and time series results as obtained from the Krylov -Bogoliubov flows in Region I (stable zone).  $A$  vs  $B$  is shown in panel (a). In panel (b),  $V_1$  vs  $V_2$  is drawn, while the time series for  $V_0$  is shown in panel (c). The parameters used in solving the flow equations are  $\Omega = 4.0$ ,  $\delta = -0.60$ ,  $\epsilon = 0.11$ ,  $\bar{\lambda} = 0.001$  (units as in Fig. 1). The oscillations are bounded with amplitudes much smaller than in Region II and similar to that in Region III.

$$\left[ \frac{\epsilon\Omega^2}{4}V_2 - \frac{3\lambda}{2}R^2 \cos 2\theta \right] V_2 - \frac{3\lambda}{2}V_1 R^2 \sin 2\theta = 0, \quad (14c)$$

$$V_2 [4\epsilon\delta\Omega + 6\lambda(R^2 + 3V_0)] = -3\lambda V_0 R^2 \sin 2\theta, \quad (14d)$$

and

$$V_1 [4\epsilon\delta\Omega + 6\lambda(R^2 + 3V_0)] + \frac{\epsilon\Omega^2}{2}V_0 = 3\lambda V_0 R^2 \cos 2\theta. \quad (14e)$$

Eliminating  $V_2$  from Eqs. (14a) and (14b), we get

$$\left[ \epsilon\delta\Omega + 3\lambda \left( V_0 + \frac{R^2}{4} \right) \right] \cos 2\theta = \frac{\epsilon\Omega^2}{8} + \frac{3\lambda}{2}V_1. \quad (15)$$

Subtracting the above from Eq. (14a) leads to

$$\left[ 3\lambda \left( V_0 + \frac{R^2}{4} \right) + \epsilon\delta\Omega \right] \sin 2\theta = -\frac{3\lambda}{2}V_2. \quad (16)$$

Using Eq. (14d) to express  $V_2$  in terms of  $V_0$ , we arrive at

$$\left[ 9(R^2 + 4V_0) + 12\frac{\epsilon\delta\Omega}{\lambda} \right] \left[ (R^2 + 3V_0) + \frac{2\epsilon\delta\Omega}{3\lambda} \right] = 9V_0 R^2. \quad (17)$$

The above equation (17) cannot be satisfied for any positive (as per requirement) value of the quantities  $R$ ,  $V_0$ ,  $\epsilon$ ,  $\delta$ ,  $\lambda$ , and  $\Omega$ . This establishes our second statement above that the classical fixed points are wiped out by quantum fluctuations in the resonance zone ( $-\Omega/8 < \delta < \Omega/8$ , Region II). As expected

the numerical  $V_2(t)$  versus  $V_1(t)$  plot in Fig. 2(b) shows erratic oscillations and so does  $V_0(t)$  versus  $t$  plot in Fig. 2(c). One should note that the amplitude of the dynamics is large (resonance), but there is no evidence of the existence of a recurrent behavior. The absence of any timescale in this dynamics, we

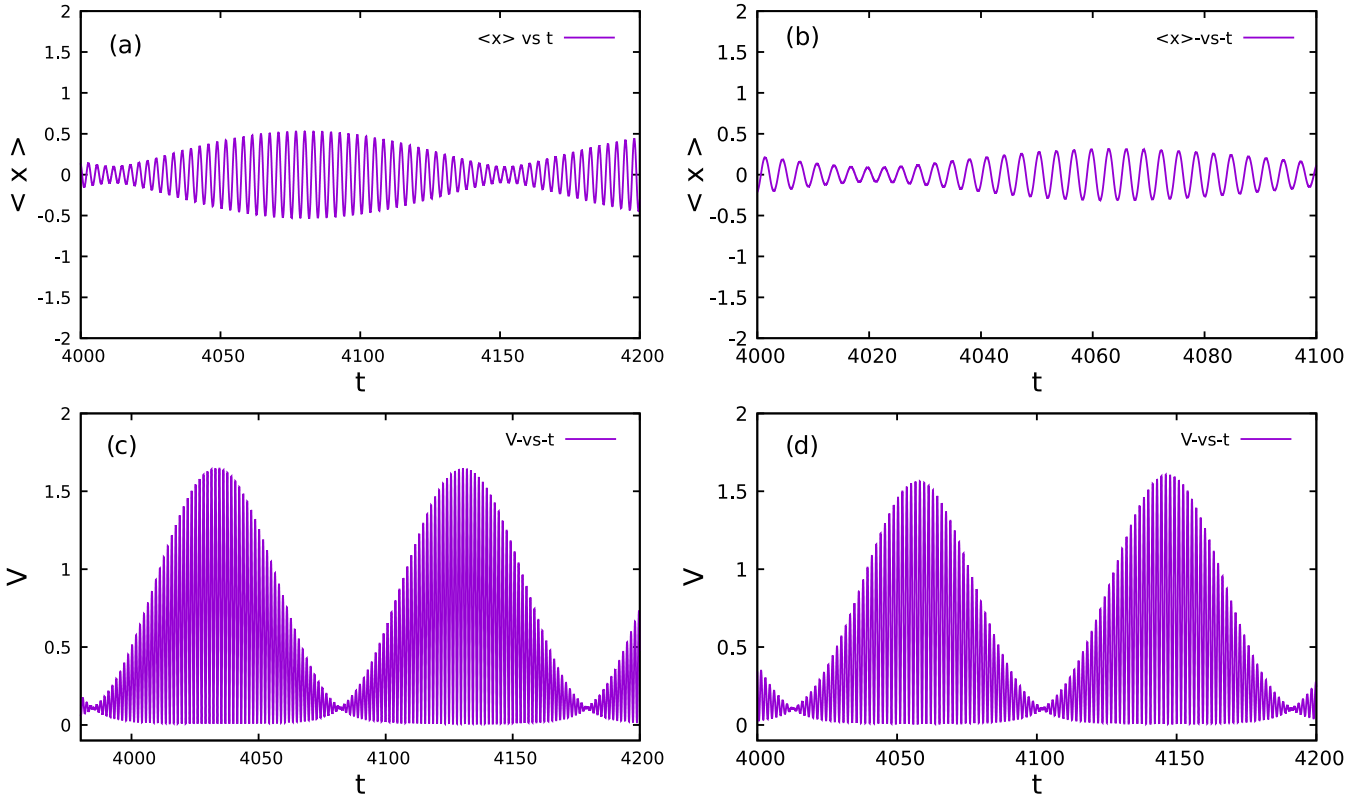


FIG. 4. Direct simulation of the coupled system constituted by Eq. (4) and Eq. (10): Time series for mean position and variance for  $\omega > \Omega/2$ . The time series are just outside the resonance zone and are shown for two values of  $\bar{\lambda}$ ,  $\bar{\lambda} = 0.001$  and  $\bar{\lambda} = 0.01$ , respectively. Panels (a) and (c) represent the variations of  $\langle x \rangle$  and  $V$  respectively for  $\bar{\lambda} = 0.001$ , whereas in panels (b) and (d) the variations of  $\langle x \rangle$  and  $V$ , respectively, have been displayed for  $\bar{\lambda} = 0.01$ . The parameters used in the simulation are  $\Omega = 4.0$ ,  $\omega = 2.06$ ,  $\epsilon = 0.11$  (units as in Fig. 1).

believe, is the dynamical system version of quantum heating. The implication of this is that the dynamics of  $\langle x \rangle(t)$  and  $V(t)$  (when the full numerical analysis is carried out in the next section) will not be periodic or even quasiperiodic in Region II. Finally, to end this section we turn to Region I, where  $\delta < -\Omega/8$ , and once again, we find bounded dynamics, quite similar to that in Region III. The corresponding figures are shown in Figs. 3(a) to 3(c).

#### IV. NUMERICAL SOLUTION

In this section, we directly integrate our Eqs. (4) and (10) to obtain the dynamics of  $\langle x \rangle$  and  $V$ . We provide initial values of  $x_0$  and  $V_0$  for  $\langle x \rangle$  and  $V$  in Eqs. (4) and (10) and carry out the numerical solution. This assumes that the initial wave packet is the Gaussian  $\frac{1}{\pi^{1/4}\sqrt{V_0}}e^{-(x-x_0)^2/2V_0}$ , and according to our assumption, it is subsequently  $\frac{1}{\pi^{1/4}\sqrt{V}}e^{-(x-\langle x \rangle(t))^2/2V(t)}$ . From our analysis of the Krylov-Bogoliubov reduction in Sec. III, we expect the dynamics will be low-amplitude almost periodic oscillations around  $\langle x \rangle = 0$  and some small time-averaged value of  $V(t)$  in Region III and Region I. In Region II we do not expect any periodic behavior since there is no fixed point at all in the Krylov-Bogoliubov approximation in this zone. We expect the amplitude of the mean position and variance to be an order of magnitude or more higher than in Regions I and III for  $\bar{\lambda} \leq 10^{-3}$  and  $\epsilon \leq 10^{-1}$ .

We begin with Region III. The basic time period for  $\langle x \rangle$  in this region  $2\pi/\omega$  and that for  $V$  is  $\pi/\omega$ . This region corresponds to  $\omega > \frac{\Omega}{2} + \frac{\epsilon\Omega}{8}$ . For our choice of  $\Omega = 4.0$ , this implies  $\omega > 2 + 0.5\epsilon$ . We have used  $\epsilon = 0.11$ , which requires  $\omega > 2.055$ . We have set  $\omega = 2.06$ , which is very close to 2.055. Our solution in this region can safely ignore the nonlinear terms in Eq. (4) when  $\bar{\lambda} = 10^{-3}$  [Figs. 4(a) and 4(c)], and we need the solution of Eq. (4) in the form  $\langle \ddot{x} \rangle + (\frac{\Omega}{2} + \epsilon\delta)^2(1 + \epsilon \cos \Omega t)\langle x \rangle = 0$ , where,  $\Omega = 4.0$ ,  $\epsilon = 0.11$ , and  $\epsilon\delta = 0.06$ . Trying a solution  $\langle x \rangle = F(t) \cos \frac{\Omega t}{2} + G(t) \sin \frac{\Omega t}{2}$ , where  $F(t)$  and  $G(t)$  are slowly varying functions, it is well known that for  $\delta > \frac{\Omega}{8} (= \frac{1}{2})$  as we have here, the amplitudes  $F(t)$  and  $G(t)$  are periodic with the period  $T = 2\pi/\epsilon\sqrt{\delta^2 - (\frac{\Omega}{8})^2}$ . Hence the solution for  $\langle x \rangle$  in this region has the form  $\langle x \rangle \propto e^{(2\pi it)/T} \cos(\frac{\Omega}{2} + \alpha)$ . The basic period is  $4\pi/\Omega = \pi$  for  $\Omega = 4.0$ , and this is seen as the rapid variation in Fig. 4(a), and the amplitude oscillates with the period  $T$  above which for  $\epsilon = 0.11$ ,  $\Omega = 4.0$ , and  $\delta = 0.06$  works out as 300 which is the time period of the modulating wave in Fig. 4(a). For Fig. 4(b), the value of  $\lambda$  is larger, and a correction to the above results from the coupling between  $\langle x \rangle$  and  $V$  would have to be included. As for  $V(t)$ , for very small values of  $\lambda$ , we can ignore the  $\lambda$  containing terms in Eq. (10), and the resulting solutions can be found in Ref. [42]. What one sees in Figs. 4(c) and 4(d) is the addition of a constant contribution and a sinusoidal variation, the constant coming from the zero

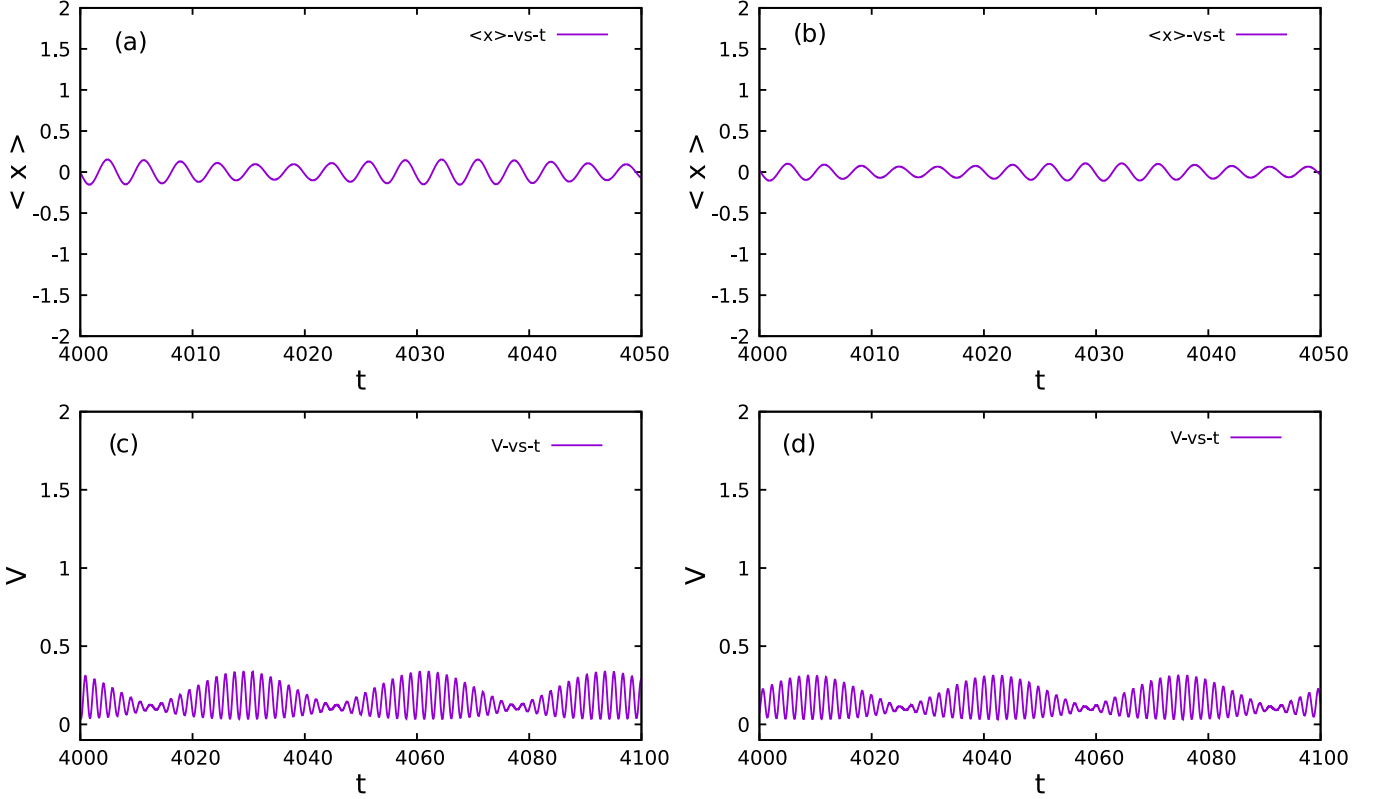


FIG. 5. Time series of  $\langle x \rangle$  and  $V$  for  $\omega < \Omega/2$  (Region I) as obtained from the direct simulation of the coupled system [Eq. (4) and Eq. (10)]. The amplitudes are much smaller in each case compared to the  $\omega = \Omega/2$  case. Keeping other parameters fixed, two different sets have been shown here, for  $\bar{\lambda} = 0.001$  and  $\bar{\lambda} = 0.01$ . Panels (a) and (c) represent the variations of  $\langle x \rangle$  and  $V$ , respectively for  $\bar{\lambda} = 0.001$ , whereas in panels (b) and (d) the variations of  $\langle x \rangle$  and  $V$ , respectively, have been displayed for  $\bar{\lambda} = 0.01$ . The used set of parameters are as follows:  $\Omega = 4.0$ ,  $\omega = 1.89$ ,  $\epsilon = 0.11$  (units as in Fig. 1).

eigenvalue in the linear part of Eq. (10). Since almost identical logic holds for Region I, we do not discuss it separately. The results are shown in Fig. 5.

We begin by trying to anticipate what the dynamics of  $\langle x \rangle$  and  $V$  will look like in Region II. From the structure of Eqs. (4) and (10) coupled with the Krylov-Bogoliubov system written in Eqs. (12) in this resonant zone for  $\bar{\lambda} \ll 1$ , we anticipate an amplitude of oscillation for  $\langle x \rangle$  [see the assumed solution in Eq. (11)], which is approximately  $O(1/\sqrt{\bar{\lambda}})$  and an amplitude for  $V$ , which is  $O(1/\bar{\lambda})$ . This would mean that the amplitude of oscillation of  $V$  will be significantly greater than the amplitude for  $\langle x \rangle$ . This is the first thing that we note from Figs. 6(a) and 6(b). For  $\bar{\lambda} \simeq 10^{-3}$ , the amplitude of oscillation for  $\langle x \rangle$  is about 20, while that for  $V$  is about 100. We note from Figs. 6(a) and 6(b) that there is a waxing and waning of the amplitude on a much larger timescale. We can actually anticipate this from Eqs. (12a) and (12b) if we ignore the coupling of  $\langle x \rangle$  and  $V$ . In that case, for  $-\frac{\Omega}{8} < \delta < \frac{\Omega}{8}$ , linearizing about the fixed point  $A^* = 0$ ,  $B^* = \pm \sqrt{\frac{4\epsilon \Delta \Omega}{3 \bar{\lambda}}}$ , with  $\Delta = \frac{\Omega}{8} - \delta$ , we find that  $\delta A = A - A^*$  and  $\delta B = B - B^*$  satisfy

$$\begin{aligned} \delta \dot{A} &= 2\epsilon \Delta \delta B, \\ \delta \dot{B} &= -\frac{\epsilon \Omega}{4} \delta A, \end{aligned}$$

leading to  $\delta \ddot{A} + \Omega_0^2 \delta A = 0$ , with  $\Omega_0^2 = \epsilon^2 \Delta \Omega / 2$ . At  $\Delta = \Omega/8$  (the value for which Fig. 6 has been drawn,  $\Omega_0^2 = \epsilon^2 \Omega^2 / 16$ ). This gives a modulation timescale of  $2\pi/\epsilon$ , which is what we see in Fig. 6(a) with  $\epsilon = 0.11$ . A similar argument qualitatively gives the modulation of the amplitude of the variance in this limit. The primary issue for such low values of  $\bar{\lambda}$  is that the dynamics of  $\langle x \rangle$  and  $V$  are extremely weakly coupled. As the value of  $\bar{\lambda}$  increases, this coupling also increases and the dynamics of  $\langle x \rangle$  starts deviating strongly from its behavior when the coupling is negligible. This is the point made in Figs. 6(c) to 6(e). Here, as we increase the value of  $\bar{\lambda}$ , the number of independent timescales appearing in  $\langle x \rangle$  starts increasing, and this is consistent with the finding of Dykman *et al.* [38], where it is seen that the driven quantum system is effectively characterized by a set of independent frequencies (incommensurate in general) and leads to the concept of quantum heating.

## V. SUMMARY

In this paper, we have looked at the nonlinear parametric oscillator in quantum mechanics. The weak quantum limit (where the variance dynamics is accurately obtained) is the approximation used to reduce the problem to a pair of coupled nonlinear ordinary differential equations for the mean position and the variance. To get an analytic handle in the physically interesting subharmonic resonance zone, we tried

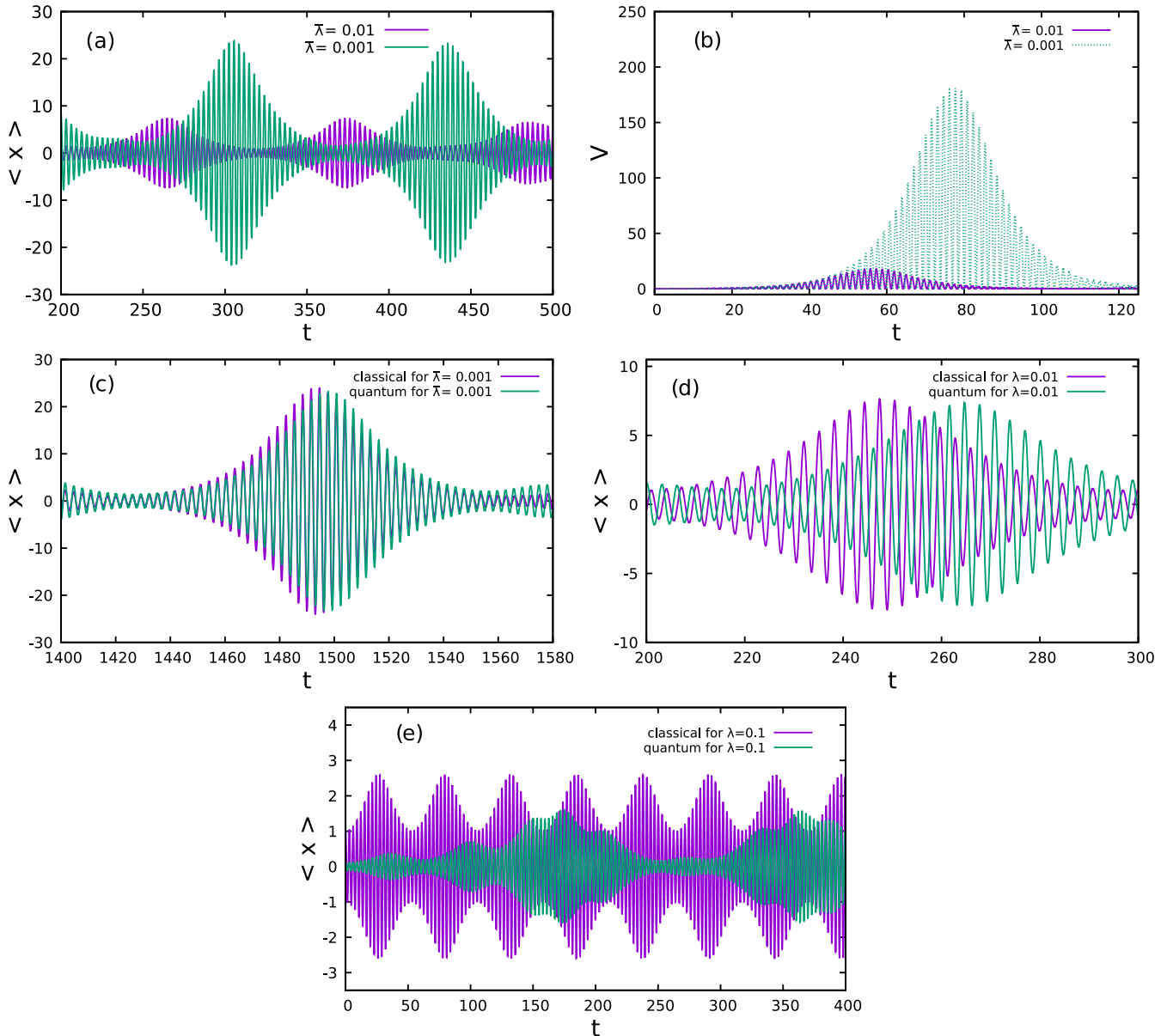


FIG. 6. The large-amplitude oscillations of the mean position and variance for  $\bar{\lambda} = 0.001$  and  $\bar{\lambda} = 0.01$  are shown in panels (a) and (b), respectively. In panels (c) to (e) the time series for the mean position  $\langle x \rangle$  has been shown for  $\bar{\lambda} = 0.001$ ,  $\bar{\lambda} = 0.01$ , and  $\bar{\lambda} = 0.1$ , for classical and quantum cases. The increasing influence of quantum fluctuation on the classical dynamics is apparent. The following set of parameters has been used:  $\Omega = 4.0$ ,  $\omega = 2.0$ ,  $\epsilon = 0.11$  (units as in Fig. 1).

the Krylov-Bogoliubov technique. The quantum fluctuations actually wipe out the classical fixed points in the resonance zone and hence in that zone perturbative techniques are of limited value. We want to focus mainly on our results shown in Fig. 6. The large quantum variance shown in Fig. 6(b) and its significant influence on the dynamics of the mean position for increasing nonlinearity as shown in Fig. 6(e) are the primary features of this present work. The dynamics of  $\langle x \rangle$  in the resonance zone is no longer characterized by a single frequency (and its harmonics) and bears a very close

resemblance to the quantum heating discussed by Dykman *et al.* [38,39].

**ACKNOWLEDGMENTS**

P.S. is grateful to Prof. Deb Shankar Ray and Shibashis Paul, SRF, for useful discussions. P.S. also thanks the Science and Engineering Research Board, Department of Science and Technology, Government of India for a J. C. Bose National Fellowship (of Prof. Deb Shankar Ray), under Grant No. SB/S2/JCB-030/2015, for partial financial support.

[1] M. DiVentra, S. Evoy, and J. R. Heflin, *Introduction to Nanoscience and Technology* (Kluwer Academic Publishers, Boston, 2004).

[2] M. R. Paul and M. C. Cross, *Phys. Rev. Lett.* **92**, 235501 (2004).

[3] C. A. Regal, J. D. Teufel, and K. W. Leihert, *Nat. Phys.* **4**, 555 (2008).

- [4] G. Anetsberger, O. Arcizet, Q. P. Unterreithmeier, R. Rivière, A. Schliesser, E. M. Weig, J. P. Kotthaus, and T. J. Kippenberg, *Nat. Phys.* **5**, 909 (2009).
- [5] L. G. Villanueva, R. B. Karabalin, M. H. Matheny, E. Kenig, M. C. Cross, and M. L. Roukes, *Nano Lett.* **11**, 5054 (2011).
- [6] I. Katz, A. Retzker, R. Straub, and R. Lifshitz, *Phys. Rev. Lett.* **99**, 040404 (2007).
- [7] L. G. Villanueva, E. Kenig, R. B. Karabalin, M. H. Matheny, R. Lifshitz, M. C. Cross, and M. L. Roukes, *Phys. Rev. Lett.* **110**, 177208 (2013).
- [8] M. G. A. Paris, M. G. Genoni, N. Shammah, and B. Teklu, *Phys. Rev. A* **90**, 012104 (2014).
- [9] B. Teklu, A. Ferraro, M. Paternostro, and M. G. A. Paris, *EPJ Quantum Technol.* **2**, 16 (2015).
- [10] D. E. Chung, K. K. Ni, O. Painter, and H. J. Kimble, *New J. Phys.* **14**, 045002 (2012).
- [11] A. H. Safavi-Naeini, J. Chan, J. T. Hill, T. P. M. Alegre, A. Krause, and O. Painter, *Phys. Rev. Lett.* **108**, 033602 (2012).
- [12] R. D. Delaney, A. P. Reed, R. W. Andrews, and K. W. Lehnert, *Phys. Rev. Lett.* **123**, 183603 (2019).
- [13] D. Leibfried, R. Blatt, C. Monroe, and D. Wineland, *Rev. Mod. Phys.* **75**, 281 (2003).
- [14] R. J. Cook, D. G. Shankland, and A. L. Wells, *Phys. Rev. A* **31**, 564 (1985).
- [15] M. Combescure, *Ann. I.H.P.: Phys. Theor.* **44**, 293 (1986).
- [16] L. S. Brown, *Phys. Rev. Lett.* **66**, 527 (1991).
- [17] R. J. Glauber, *Laser Manipulation of Atoms and Ions*, “Enrico Fermi” Course 118 (North-Holland, Amsterdam, 1999).
- [18] D. W. Jordan and P. Smith, *Nonlinear Ordinary Differential Equations*, 4th ed. (Oxford University Press, Oxford, 2007).
- [19] S. Wirkus, R. Rand, and A. Ruina, *Coll. Math. J.* **29**, 266 (1998).
- [20] K. L. Turner, S. A. Miller, P. G. Hartwell, N. C. MacDonald, S. H. Strogatz, and S. G. Adams, *Nature (London)* **396**, 149 (1998).
- [21] R. Lifshitz and M. L. Roukes, *Phys. Rev. B* **61**, 5600 (2000).
- [22] B. Ilic, S. Krylov, K. Aubin, R. Reichenbach, and H. G. Craighead, *App. Phys. Lett.* **86**, 193114 (2005).
- [23] S. S. Verbridge, L. M. Bellan, J. M. Parpaia, and H. G. Craighead, *Nano Lett.* **6**, 2109 (2006).
- [24] B. E. DeMartini, J. F. Rhoads, K. L. Turner, S. W. Shaw, and J. Moehlis, *J. Microelectromechanic. Sys.* **16**, 310 (2007).
- [25] B. E. DeMartini, H. E. Butterfield, J. Moehlis, and K. L. Turner, *J. Microelectromechanic. Sys.* **16**, 1314 (2007).
- [26] J. F. Rhoads, S. W. Shaw, K. L. Turner, J. Moehlis, B. E. DeMartini, and W. Zhang, *J. Sound Vib.* **296**, 797 (2006).
- [27] E. Buks and M. L. Roukes, *Europhys. Lett.* **54**, 220 (2001).
- [28] R. Lifshitz and M. C. Cross, *Reviews of Nonlinear Dynamics and Complexity*, Vol. 1 (Wiley-VCH, 2008).
- [29] J. F. Rhoads, S. W. Shaw, and K. L. Turner, *J. Dyn. Sys. Meas. Control* **132**, 034001 (2010).
- [30] A. M. Perelomov and V. S. Popov, *Teor. Mat. Fiz.* **1**, 275 (1969).
- [31] K. Husimi, *Prog. Theor. Phys.* **9**, 381 (1953).
- [32] J. Rezende, *J. Math. Phys.* **25**, 3264 (1984).
- [33] P. S. Riseborough, P. Hänggi, and U. Weiss, *Phys. Rev. A* **31**, 471 (1985).
- [34] R. Graham and H. Haken, *Z. Phys.* **210**, 276 (1968).
- [35] H. J. Carmichael and M. Wolinsky, in *Quantum Optics IV*, edited by J. D. Harvey and D. F. Walls (Springer-Verlag, Berlin, 1986), pp. 208–220.
- [36] P. Kinsler and P. D. Drummond, *Phys. Rev. A* **43**, 6194 (1991); **52**, 783 (1995).
- [37] S. Ding, G. Maslennikov, R. Hablützel, H. Loh, and D. Matsukevich, *Phys. Rev. Lett.* **119**, 150404 (2017).
- [38] M. I. Dykman, M. Marthaler, and V. Peano, *Phys. Rev. A* **83**, 052115 (2011).
- [39] V. Peano and M. I. Dykman, *New J. Phys.* **16**, 015011 (2014).
- [40] S. Biswas, R. Chattopadhyay, and J. K. Bhattacharjee, *Phys. Lett. A* **382**, 1202 (2018).
- [41] V. Grubelnik, M. Logar, M. Robnik, and Y. Xia, *Phys. Rev. E* **99**, 022209 (2019).
- [42] S. Biswas and J. K. Bhattacharjee, *Nonlinear Dyn.* **96**, 737 (2019).
- [43] S. Bhattacharjee, D. S. Ray, and J. K. Bhattacharjee, *J. Math. Chem.* **50**, 819 (2012).
- [44] R. S. Zounes and R. H. Rand, *Int. J. Nonlinear Mech.* **37**, 43 (2002).
- [45] L. D. Landau and E. M. Lifshitz, *Mechanics* (Pergamon Press, Oxford, 1982), Chap. 6.
- [46] S. H. Strogatz, *Nonlinear Dynamics and Chaos: With Applications to Physics, Biology, Chemistry and Engineering* (Westview Press, Denver, 2015), Chap. 6.
- [47] R. H. Rand, *Lecture Notes on Nonlinear Vibrations*, version 53 (Cornell University, Ithaca, NY, 2012).
- [48] E. J. Heller, *J. Chem. Phys.* **62**, 1544 (1975).
- [49] A. K. Pattanayak and W. C. Schieve, *Phys. Rev. Lett.* **72**, 2855 (1994); *Phys. Rev. E* **50**, 3601 (1994).
- [50] B. Sundaram and P. W. Milonni, *Phys. Rev. E* **51**, 1971 (1995).
- [51] L. E. Ballentine and S. M. McRae, *Phys. Rev. A* **58**, 1799 (1998).
- [52] T. Bhattacharya, S. Habib, and K. Jacobs, *Los Alamos Sci.* **27**, 110 (2002).
- [53] D. Brizuela, *Phys. Rev. D* **90**, 125018 (2014).
- [54] R. Chawla and J. K. Bhattacharjee, *Eur. Phys. J. B* **92**, 196 (2019).
- [55] I. Katz, R. Lifshitz, A. Retzker, and R. Straub, *New J. Phys.* **10**, 125023 (2008).
- [56] M. I. Dykman and V. N. Smelyanskii, *Zh. Eksp. Teor. Fiz.* **94**, 61 (1988) [*Sov. Phys. JETP* **67**, 1769 (1988)].
- [57] M. I. Dykman, *Phys. Rev. E* **75**, 011101 (2007).
- [58] M. Marthaler and M. I. Dykman, *Phys. Rev. A* **73**, 042108 (2006).